Glia-independent chains of neuroblasts through the subcortical parenchyma of the adult rabbit brain.

Glia-independent chains of neuroblasts through the subcortical parenchyma of the adult rabbit brain

F. Luzzati[*], P. Peretto[*], P. Aimar[†], G. Ponti[†], A. Fasolo[*‡], and L. Bonfanti[†‡§]

[*]Department of Animal and Human Biology, University of Turin, Via Accademia Albertina 13, 10153 Turin, Italy; [†]Department of Veterinary Morphophysiology, University of Turin, Via Leonardo da Vinci 44, 10095 Grugliasco (TO), Italy; and [‡]Rita Levi Montalcini Center for Brain Repair, 10125 Turin, Italy

In the brains of adult mammals long-distance cell migration of neuronal precursors is known to occur in the rostral migratory stream, involving chains of cells sliding into astrocytic glial tubes. By combining immunocytochemistry for polysialylated neural cell adhesion molecule (PSA-NCAM), neuronal and glial antigens, endogenousm and exogenously administered cell-proliferation markers, and light and electron microscopy 3D reconstructions, we show that chains of newly generated neuroblasts exist both inside and outside the subventricular zone of adult rabbits. Two groups of chains were detectable within the mature brain parenchyma: anterior chains, into the anterior forceps of the corpus callosum, and posterior chains, close to the external capsule. Parenchymal chains were not associated with any special glial structures, thus coming widely in contact with the mature nervous tissue, including unmyelinatedmyelinated fibers, astrocytes, neurons, and oligodendrocytes. These chains of cells, unlike those in the subventricular zone, do not display cell proliferation, but they contain BrdUrd administered several weeks before. Telencephalic areas, such as the putamen, amygdala, claustrum, and cortex, adjacent to the chains harbor numerous PSA-NCAM-positive cells. The counting of newly generated cells in these areas shows small differences in comparison with others, and a few cells double-labeled for BrdUrd/PSA-NCAM (after 1-month survival) and for BrdUrd/NeuN (after 2 months) were detectable. These results demonstrate the occurrence of glial-independent chains of migrating neuroblasts, which directly contact the mature brain parenchyma of adult mammals. These chains could provide a possible link between the adult germinative layers and a very low-rate/long-term process of cell addition in the telencephalon.

Crucial morphogenetic processes, such as cell proliferation and migration, commonly occur during developmental early postnatal periods, but they are highly restricted in the adult brain. In mammals, adult neurogenesis has been fully demonstrated to occur in two allocortical (three-layered) regions: the hippocampus (1) and the olfactory bulb (2). At present, the only well characterized example of long-distance cell migration in the adult mammalian brain is the rostral migratory stream (RMS), allowing the displacement of cell precursors from the forebrain subventricular zone (SVZ) to the olfactory bulb (2). This unique type of migration consists of tangentially oriented ''chains'' of cells expressing the polysialylated form of the neural cell adhesion molecule (PSA-NCAM; refs. 3 and 4) and sliding into a meshwork of astrocytic ''glial tubes'' (5, 6). Recent studies carried out in primates, in addition to the RMS (7, 8), reported the existence of newly generated neurons in several telencephalic areas, including the neocortex and the amygdala (9–11). Although a stream of proliferating cells was observed between the lateral ventricle and the amygdala (11), and some elongated cells were detected in the white matter beneath cortical areas (9), these studies did not provide conclusive evidence concerning the migratory pathway to these areas. Thus, the question remains whether chain migration within astrocytic glial sheaths is the unique device allowing long-distance cell displacement into the intact mature mammalian brain. Starting from the hypothesis that

Abbreviations: RMS, rostral migratory stream; SVZ, subventricular zone; PSA-NCAM, polysialylated neural cell adhesion molecule; RE, rostral extension; VLE, ventral-lateral extension; GFAP, antiglial fibrillary acidic protein.

[§]To whom correspondence should be addressed. E-mail: luca.bonfanti@unito.it.

adult neurogenesis and the organization of cerebral ventricles can vary across mammalian species in relation to the different brain anatomy and functions (12, 13), we have analyzed the SVZ and its extensions in the adult rabbit brain, where an olfactory ventricle persists in the area corresponding to the rodent's RMS, and the lateral ventricle is more expanded posteriorly (14). Using electron microscopy, we show here the existence of chains of migrating cells leaving the SVZ to enter the mature brain parenchyma without being in contact with any specialized glial structures. These chains run tangentially to the external capsule, through peristriatal and subcortical areas, which also contain newly generated cells.

Materials and Methods

BrdUrd Injections and Tissue Preparation. Experiments were conducted in accordance with current European Union and Italian law, under authorization of the Italian Ministry of Health, no. 66/99-A. Twenty-two adult (3–6 months old) New Zealand White HY/CR rabbits (*Orictolagus cuniculus*; Charles River, Milan) received i.p. injections of BrdUrd (Sigma; 40 mg/kg of body weight in 0.1 M Tris). Eight rabbits were killed 2 h after a single BrdUrd injection. Twelve rabbits received daily injections of BrdUrd for 5 days and were killed 2 h, and 5, 10, 30, and 60 days after the last injection. Animals were anesthetized (pentothal sodium) and perfused intracardially with a heparinized saline solution followed by 4% paraformaldehyde plus 2% picric acid (light microscopy) or 2% glutaraldehyde plus 1% paraformaldehyde (electron microscopy) in 0.1Msodium phosphate buffer, pH 7.4. Brains for light microscopy were postfixed overnight, cryoprotected, frozen at -80°C, and cryostat (25 and 40 μm)- or vibratome-sectioned in series. Brains for electron microscopy were postfixed 2 h, and then coronal vibratome sections (200 μm) were cut, fixed in osmium ferrocyanide for 1 h, stained *en bloc* with 1% uranyl acetate, dehydrated, and embedded in Araldite (Fluka, Buchs, Germany) (6). Ultrathin sections were examined with a Philips CM10 transmission electron microscope.

Immunohistochemistry. Immunohistochemistry was carried out by using single-peroxidase and double-immunofluorescence methods on cryostat sections incubated overnight at 4°C. The following primary antisera and antibodies were used: (i) anti-PSA-NCAM, diluted 1:4,000 (monoclonal IgM; G. Rougon, Marseille); (ii) anti-BrdUrd, 1:2,000 (monoclonal, Harlan Laboratories, Haslett, MI); (iii) anti-Ki67, 1:300 (MIB1, monoclonal, Immunotech, Luminy, France); (iv) anti-class III β-tubulin, 1:600 (TU-J1, monoclonal and polyclonal, Babco, Richmond, VA); (v) antiglial fibrillary acidic protein, 1:1,000 (GFAP, polyclonal, DAKO); (vi) anti-vimentin, 1:800 (monoclonal, DAKO); (vii) anti-human neuronal protein HuCD, 1:200 (monoclonal, Molecular Probes); (viii) anti-NeuN, 1:1,000 (monoclonal, Chemicon). For double staining, a combination of two indirect immunofluorescence procedures using FITC and rhodamine or FITC and Cy3-conjugated antibodies were used. All antibodies were diluted in 0.01 M PBS containing 0.1% Triton X-100. Fluorescent specimens mounted in 1,4-diazabicyclo[2.2.2]octane (Dabco, Sigma) were observed with a laser-scanning Olympus Fluoview confocal system (Olympus, New Hyde Park, NY).

Light and Electron Microscopic 3D Reconstructions. Serial cryostat coronal sections (40 μm) were used for 3D reconstructions in light microscopy. Thirty representative sections taken at 320-μm intervals were used to delineate the SVZ area. Thirty and 90 serial sections immunostained for PSA-NCAM were used to obtain 1.2- and 3.6-mm total reconstructions of the anterior and posterior chains, respectively. The electron microscopic reconstruction of a posterior chain of cells was carried out on serial ultrathin sections (80 nm thick) collected onto Formvar-coated grids. Micrographs from the tenth section in the sequence were drawn to define the contour of single cells. The digital images were added in sequence in PHOTOSHOP (Adobe Systems, Mountain View, CA), and the contours imported to RHINO 3D software (Robert McNeel & Associates, Seattle). Drawings from 30 levels (15 levels shown in Fig. 3) were examined to follow the evolution of the chain across a total length of 24 μm. The levels from 4 to 20 were analyzed every fifth section (spaced 0.4 nm) at a

higher magnification to obtain a 3D reconstruction of single cells.

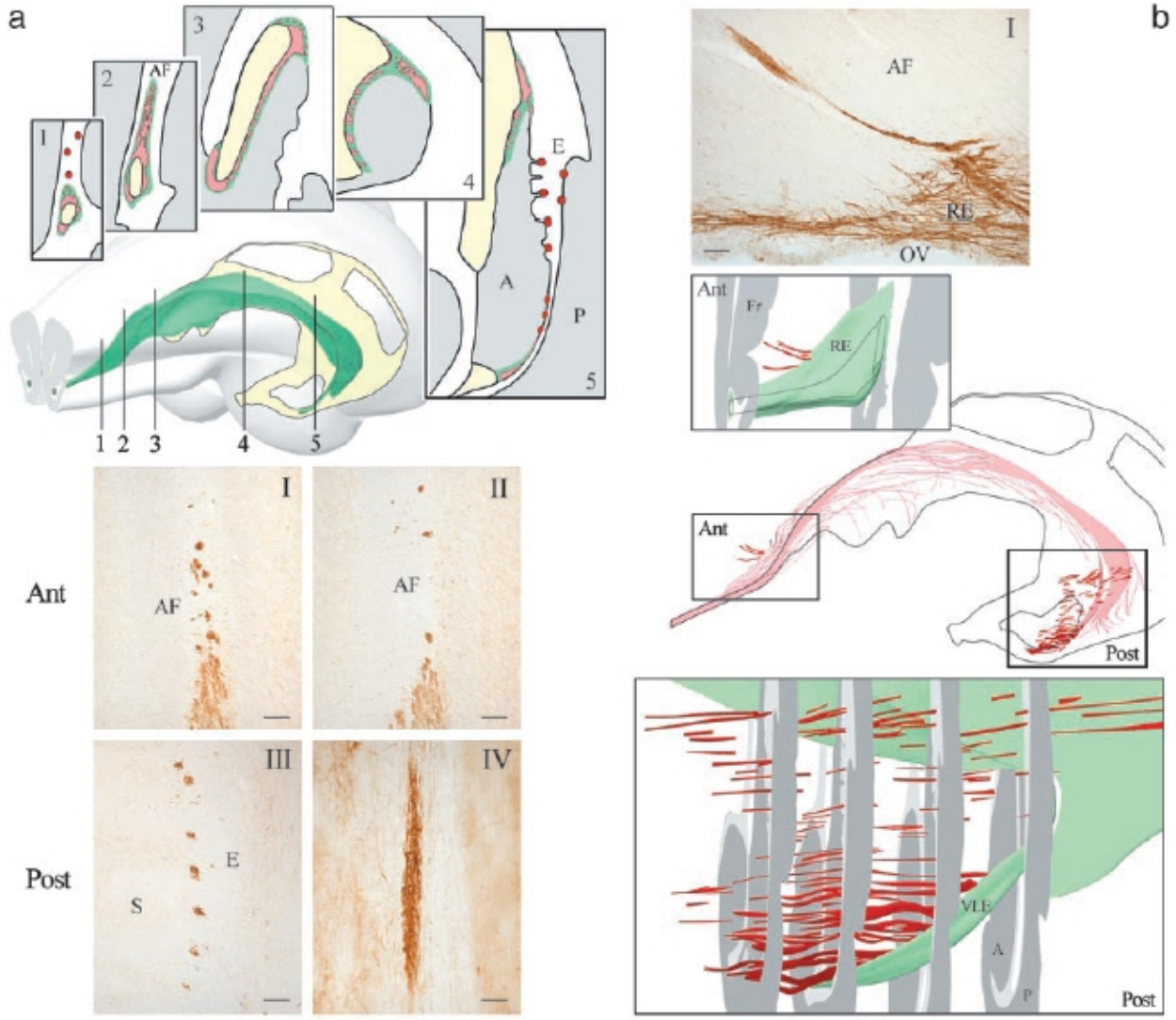

Fig. 1. Organization of the adult-rabbit SVZ and its extensions. (a) 3D reconstruction of the SVZ (green) over the ventricles (yellow). Representative coronal sections (1–5) show the SVZ internal organization: glial densities (green) and PSA-NCAM-immunoreactive chains and masses of cells (pink). Coronal (I–III) and horizontal (IV) sections revealing PSA-NCAM$^+$ an terior (Ant) and posterior (Post) chains into the mature brain parenchyma. Their position is indicated by red dots in schematic sections 1 and 5. (b *Middle*) Distribution of PSA-NCAM$^+$ masses and chains of cells into (pink) and outside (red) the SVZ. Serial 3D reconstruction of anterior (Ant) and posterior (Post) chains located outside the SVZ area (green), at the level of the rostral extension (RE) and ventral-lateral extension (VLE). Chains connected with the dorsal part of the RE are immersed into the white matter of the anterior forcep (AF) of the corpus callosum (in b, I, a sagittal section immunostained for PSA-NCAM). (a, III and IV) Chains from the VLE, regularly arranged between the external capsule (E) and the striatum (S). A, amygdala; P, cortex; OV, olfactory ventricle. (Bars: a, I–III, 45 μm; a, IV, 20 μm; b, 80 μm.)

Cell Counting. The number of newly generated cells (density of Ki67- and BrdUrd-immunoreactive nuclei per mm3, the latter at 2-h, 5-day, and 35-day survival times) was analyzed within two levels of the SVZ (the lateral ventricle, from the septum anterior limit, and rostral extension (RE), from the posterior limit of the anterior olfactory nucleus), in the olfactory bulb granular layer, in areas of the basal ganglia (posterior putamen, lateral amygdala) and of the temporal cortex (posterior piriform cortex, perirhinal cortex, claustrum) close to posterior parenchymal chains, and in areas not related to the chains (anterior piriform cortex, insula, anterior claustrum). Six sections cut

at 300-μm intervals, imported into PHOTOSHOP and IMAGE PROPLUS, were analyzed in each animal (n = 12).

Table 1. Morphological, cytological, and immunocytochemical features displayed by chains of cells in the adult rabbit brain shared with SVZ chains of rodents

Tangentially oriented bulks of cells (PSA-NCAM$^+$, β-tubulin$^+$, Hu$^+$, GFAP$^-$, vimentin$^-$)
Immersed in an astrocytic meshwork (GFAP$^+$, vimentin$^+$)
Morphology of migrating cells and cytology of neuroblasts
BrdUrd/PSA-NCAM simultaneous labeling at different postinjection survival times

See refs. 3–6, 15, 16, and 18.

Results

Cell Proliferation and Chain Migration in the SVZ of the Adult Rabbit. By using a combination of histological, immunocytochemical, and electron microscopic techniques, the entire SVZ area, characterized by high-cell proliferation, densely packed astrocytic cells immunoreactive for GFAP and vimentin, and tangentially oriented chains of PSA-NCAM-immunoreactive cells, was delineated along the olfactory and lateral ventricular system of the rabbit (Figs. 1 and 4). Both the main cell compartments previously described in rodents, namely the migrating neuroblasts and the astrocytic meshwork, were present in the rabbit SVZ. The RE, laying on the ependyma of the olfactory ventricle, was particularly pronounced in its dorsal part. The SVZ of the lateral ventricle was enlarged in its posterior part adjacent to the inferior horn of the ventricle, forming a ventral-lateral extension (VLE) at the limit between the striatumamygdala and the external capsule (Fig. 1). In all these areas electron microscopy confirmed the occurrence of chains of cells with the typical morphology and cytology of migrating elements described in the SVZ of rodents (Table 1). An analysis of cell proliferation was carried out in this area by using the endogenous marker Ki67 and exogenously administered BrdUrd in animals that survived 2 h, 5 days, and 35 days after the first of five daily injections. A high number of positive nuclei, frequently double-stained with the cells of the chains (Fig. 4), were observed in the anterior lateral ventricle and RMS. A significant increase in the number of newly generated cells which survived from 5 to 35 days was detected in the RE and olfactory bulb (Fig. 2 a and b), being consistent with the existence of rostralward ''chain'' migration in all mammalian species. In the posterior SVZ a high density of BrdUrd nuclei was detectable at all survival times (not shown), whereas only scattered nuclei were seen in the VLE (Fig. 4). A major difference from the pattern known in rodents emerged after detailed reconstructions in these areas, leading to the detection of chains of PSA-NCAM-immunoreactive cells leaving the SVZ.

Glial-Independent Chains of Neuroblasts Are Present in the Mature Brain Parenchyma. A light microscopic serial reconstruction, carried out on sections immunostained for PSA-NCAMtaken at the level of the RE and VLE, revealed groups of chains localized outside the SVZ area (Fig. 1). About five to six chains were observed into the anterior forceps of the corpus callosum beneath the frontal cortex, and a considerably higher number of chains (up to 40–50) were present along the external capsule (Fig. 1). The posterior chains were tangentially oriented and regularly arranged along an area 3 mm high and 3–4 mm long between the striatumamygdala and the claustrum/piriformperirhinal cortices. All the chains, both inside and outside the SVZ, shared many immunocytochemical and cytological features with those described in the rodent SVZ (Table 1), including β-tubulin and Hu protein immunoreactivity (Fig. 4). Electron microscopy confirmed that all of the cells in the parenchymal

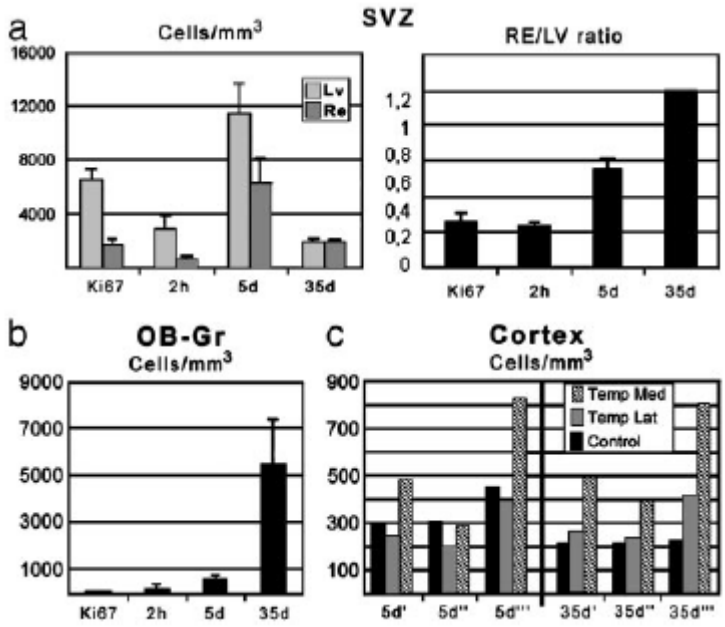

Fig. 2. Newly generated cells in the SVZ and olfactory bulb, areas adjacent to and far from the posterior parenchymal chains. (a Left) Cell proliferation within two levels of the SVZ: lateral ventricle (LV) and rostral extension (RE). (a Right) The RE/LV ratio increase at progressive survival times indicates a rostralward migration. (b) An even greater increase is detectable in the olfactory bulb granular layer (OB-Gr) . (c) $BrdUrd^+$ nuclei in areas of the basal ganglia and cortex adjacent to the posterior parenchymal chains (Temp) and in distant cortical areas (Control), at 5 and 35 days of survival, in each of six animals.

chains displayed the cytological features of migrating neuroblasts, with a large nucleus and a very thin halo of cytoplasm enriched in ribosomes (Fig. 3). After ultrastructural serial reconstruction of single cells in the chain (Fig. 3b), the typical bipolar-shaped morphology of migrating neuroblasts, with an ellipsoid cell body and leading/trailing processes on its opposite sides, was recognizable.
In addition, the parenchymal chains also showed important differences (Table 2). Simultaneous PSA-NCAM/GFAP stainings indicated no particular relationships with any special astrocytic glial structures, the chains being surrounded by the normal pattern of distribution of glial cells in white and gray matter (Fig. 4). Electron microscopy clearly showed that these chains were directly immersed in the mature parenchyma, with occasional contacts with isolated astrocytes (Fig. 3). The anterior chains were utterly immersed in unmyelinated and myelinated axons, whereas the posterior chains were also seen in contact with neurons and oligodendrocytes. In both cases, most of the chain surfaces were in direct contact with longitudinally oriented axons (Fig. 3). A difference was observed concerning the relationships among cells in the anterior and posterior chains, affecting their overall morphology. The anterior chains displayed a compact, cylindrical aspect, similar to the SVZ chains from all species, whereas the cells in the VLE chains formed multiple bulks and clusters or frequently displayed a laminar arrangement (Fig. 3). The ultrastructural serial reconstruction of a chain of the latter type revealed that small clusters and rows of cells partially disaggregate and reaggregate as the chain progresses through the tissue, most of the elements keeping their mutual contacts (Fig. 3a).

Table 2. Features of parenchymal chains

	Anterior chains	Posterior chains
Aspect	Compact, cylindrical	More dispersed, laminar
Contacts	Axons (occasional astrocytes)	Axons (occasional astrocytes, neurons, oligodendrocytes)

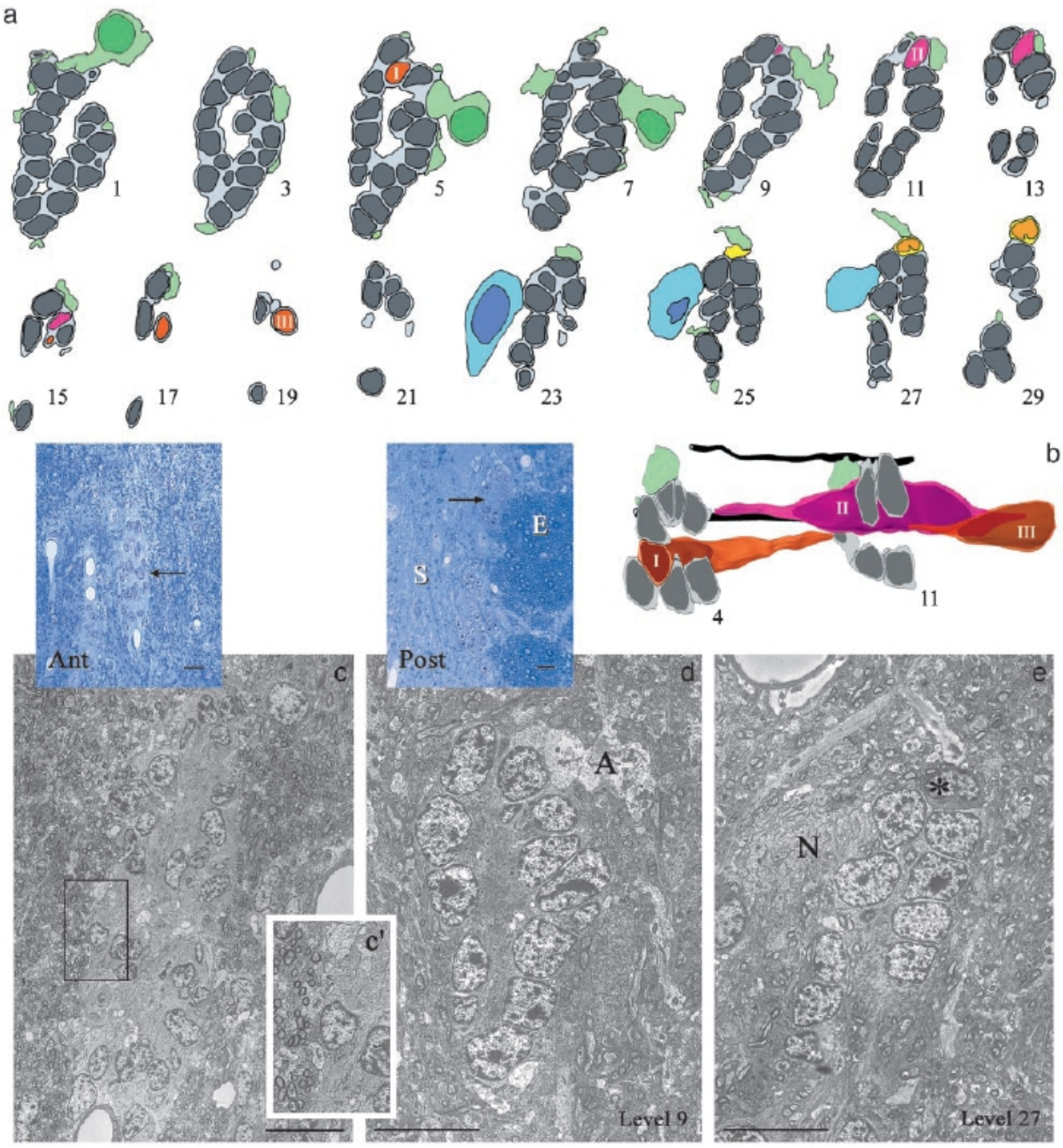

Fig. 3. Ultrastructure of parenchymal chains. (a) Reconstruction of a 24-μm tract of a posterior chain (15 of 30 levels shown). A row of cells forms a C-shaped monolayer open on one side (level 1), then forms a ring (levels 3–7); the lamina is open again on one side, then spliced in two (levels 9 and 11–21). It contains only three cell bodies at level 19. Contacts with astrocytes (green), a neuron (blue), and an oligodendrocyte (yellow) are rare, most of the chain contacting axons (not in color). (b) 3D reconstruction of cells (I–III) in the chain. Note the bipolar shape characteristic of migrating cells, with leading/trailing processes squeezed among cell bodies; in black are two myelinated axons. Semithin sections of the anterior (Ant) and posterior (Post) chains (arrows) showed in the electron micrographs (c–e). Shown in c is a detail at the interface with axons. (d and e) Two levels of the reconstructed chain. S, striatum; E, external capsule; A, astrocyte; N, neuron; asterisk, oligodendrocyte. (Bars: Ant, Post, and c, 8 μm; d and e, 4 μm.)

Cells in the Parenchymal Chains and in the Adjacent Brain Areas Are Newly Generated. The analysis of cell proliferation, carried out for Ki67 antigen or BrdUrd at 2 h after injection, revealed no immunoreactive nuclei in the parenchymal chains. By contrast, some $BrdUrd^+$ nuclei were observed in these chains at 5 days of survival, and, more frequently at 10, 15, and 35 days (Fig. 4). In ad-

dition, many PSA-NCAM-positive cells were found in the adjacent brain areas. Most of them were observed close to the chains emerging from the VLE (Fig. 4), namely in the putamen, amygdaloid lateral nucleus, posterior claustrum, posterior piriform cortex, and perirhinal cortex, and, to a lesser extent, in the frontal cortex close to the RE (not shown). These cells, either isolated or forming small aggregates, showed the typical bipolarshaped morphology of migrating elements, but were mostly radially oriented. At 35 days of survival, some BrdUrd/PSA-NCAM double-stained cells were detectable in the areas surrounding the chains (Fig. 4). After counting the number of BrdUrd$^+$ nuclei in these areas at 5 and 35 days of survival (which received equal BrdUrd injections), significant differences were not found. Nevertheless, the data obtained in the areas of the chains at 35 days were higher than those obtained in cortical areas located far from them, which revealed unvaried or decreased numbers of newly generated cells (Fig. 2c). Two months after the BrdUrd treatment, although the number of newly generated cells was very low and no BrdUrdPSA-NCAM cells were found, some BrdUrd/NeuN double-stained cells were detectable (Fig. 4).

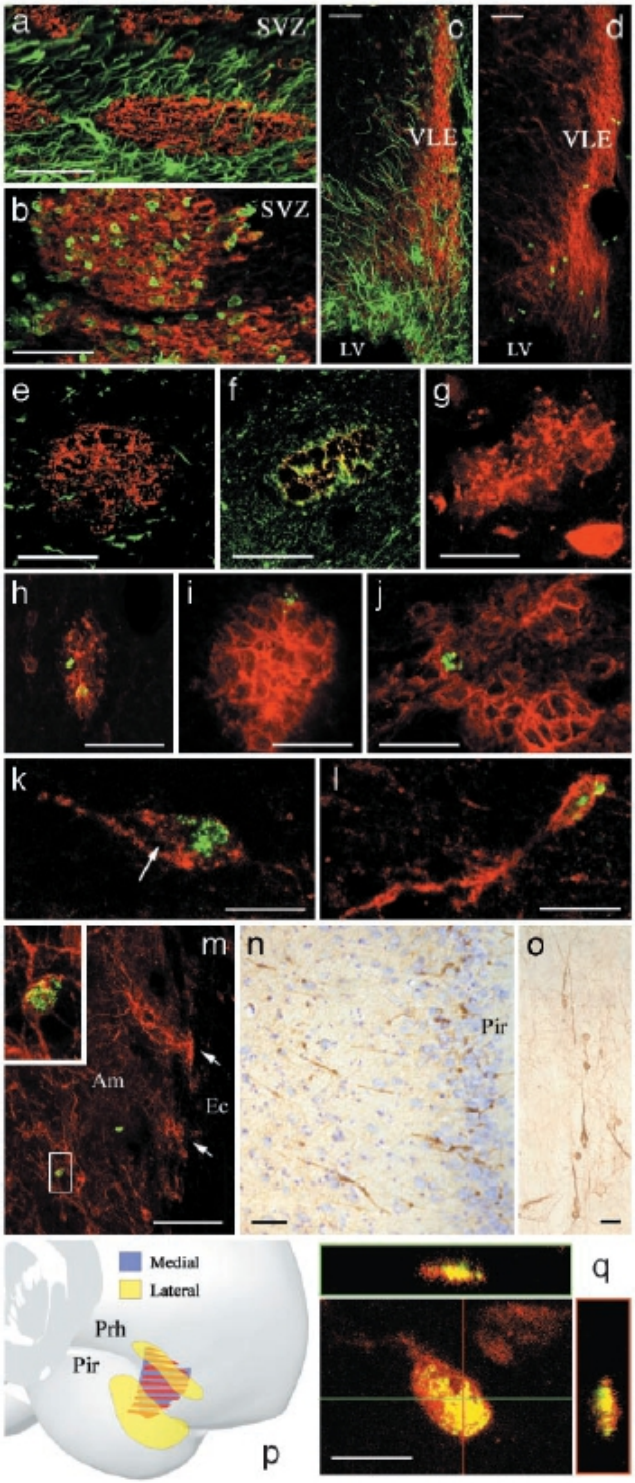

Fig. 4. Immunocytochemical characterization of the adult-rabbit SVZ, parenchymal chains, and newly generated cells. In the SVZ, PSA-NCAM$^+$ chains of cells (red) are surrounded by astrocytes (a, GFAP, green) and contain many BrdUrd$^+$ cells (b, green) after five daily injections. In the VLE (c and d), PSA-NCAM$^+$ chains (red) associated to vimentin $^+$glial structures (c, green) contain fewer BrdUrd$^+$ nuclei (d, green) after five daily injections (compare with b). Posterior parenchymal chains (e–j and m), revealed with PSA-NCAM (red, e, f, and h–j), are not ensheathed by astrocytes (e, GFAP, green), display β-tubulin (f, green) and Hu (g, red) immunoreactivity, and contain newly generated cells (BrdUrd, green, 10 and 35 days of survival; h, anterior; i and j, posterior). (k and /) Bipolar-shaped (k) and neuronal-shaped (/) PSA-NCAM$^+$ (red)/BrdUrd$^+$ (green, one negative, arrow) cells, in putamen and perirhinal cortex (35 days of survival). (m) Chains dispersed toward the amygdala (Am), with a newly generated cell (BrdUrd, green); Ec, external capsule. (n) PSA-NCAM$^+$ cells (brown) radially oriented toward the posterior piriform cortex (Pir). (o) Single, bipolar-shaped cells. (p) Schematic drawing of the areas harboring PSA-NCAM$^+$, radially oriented cells, and their spatial relationship with parenchymal chains (red); Prh, perirhinal cortex. (q) BrdUrd/NeuN double-labeled cells in the putamen. (Bars: a–d, h, and m, 50 μm; e–g, i, and j, 25 μm; k, l, n, and q, 12.5 μm; o, 6 μm.)

Discussion

Consistent cell displacement in the adult mammalian brain was not considered possible until the demonstration of long-distance migration of neuronal precursors into the RMS of rodents (2). Such migration, also described at the light microscopic level in microsmatic primates (7, 8), involves tangentially oriented chains of cells which slide into astrocytic glial tubes (5–7, 15, 16). The migrating cells have been identified as a population of β-tubulinpositive neuroblasts (17), showing specific cytological features (5, 6, 15, 16, 18) and expressing PSA-NCAM(3, 4). In this study, the same type of cells and chains were found in the rabbit SVZ, which was also a site of intense cell proliferation, the chains themselves containing newly generated cells and displaying a rostralward migratory pattern in animals treated with BrdUrd at different survival times. This finding confirms that chain migration in the SVZ toward the olfactory bulb is a common process in adult mammals, independently from differences concerning the brain anatomy of the species. Besides these similarities with rodents, some remarkable differences were observed in the rabbit SVZ. The RE was particularly expanded dorsally to the open olfactory ventricle, and a VLE was detectable along the inferior horn of the lateral ventricle. The VLE appears to be a homologue of the ‘‘temporal stream’’ described in monkeys by Bernier et al. (11). According to our study, also based on the detection of vimentin-positive astrocytes, the rabbit VLE must be considered as an SVZ extension. Apart from differences in SVZ anatomy in the rabbit, large chains of cells were detected outside this area. Several data concur to demonstrate that the cells forming these chains are analogues of the migrating neuroblasts described in rodents. First, the strong expression of polysialic acid on tangentially oriented bulks of cells is a major feature of the characteristic ‘‘chain migration’’ (3, 4). Second, the immunocytochemical expression of class III β-tubulin and Hu protein, and the incorporation of BrdUrd in elements of the chains several weeks after its administration, attest to the features of newly generated neuroblasts (15, 17, 19). Third, these cells display the morphology and cytology proper of migrating cells (5, 6), and the ultrastructural reconstruction revealed in detail their mutual relationships to form continuous chains.

Hence, the chains of cells outside the SVZ area could actually represent a temporal migration pathway toward striatal/subcortical regions. These results address two important issues: (i) the possibility that chain migration can occur through the mature parenchyma of an intact mammalian brain, and (ii) the existence of a link for possible neurogenesis in adult brain areas different from the olfactory bulb and hippocampus. Here, we focused mainly on the first issue, an element not discussed previously being the evidence for direct contact between the chains and the mature tissue, including unmyelinated myelinated axons, neurons, astrocytes, and oligodendrocytes. At least two main types of chains were observed: compact chains, similar to those in the RMS, and laminar chains. In both cases the interposition of any specialized glial structures was not observed. Previous in vitro studies showed that chain migration can occur in a glial-independent way (20), supporting the view that it is a community effect independent of environmental cues. Our serial reconstruction of a laminar chain clearly indicated how the cells can change their relative position in the chain and their relationships with the substrate during the advancement, yet not lose their mutual contact. Thus, the present study does show in vivo that a chain of neuroblasts can occur through the normal mammalian brain, not being limited to specialized pathways such as the glial tubes of the RMS. Nonetheless, the different cell aggregations observed in parenchymal chains and the pattern of distribution of their BrdUrd cells at different survival times suggest that at least the shape of the chain and the rate of migration could be affected by the substrates encountered. At the light microscopic level these chains were observed for considerable distances (up to 1 mm), showing different degrees of cell dispersion, and electron microscopy confirmed that they can be reduced to a few cells in some tracts, and then again harbor a higher number of elements. Accordingly, the temporal pattern of detection of newly generated cells in the posterior part of the SVZ, indicating an accumulation rather than a decrease at long survival times, and the absence of local cell proliferation in the parenchymal chains, strongly suggest that such migration could be discontinuous and slow if compared with the RMS. The light modifications in the number of BrdUr-dpositive nuclei observed in cortical regions

at different survival times, and the difficulty in obtaining a high number of doublestainings in these areas, could be linked to a very low rate of cell migration affecting a small number of cells across wide brain regions. Nevertheless, the low doses of BrdUrd used here in comparison with previous reports (9, 10) could lead to an underestimation of the actual degree of cell genesis. Indeed, it has been shown that BrdUrd can be administered up to 300 mg/kg, lower doses labeling only a fraction of the S-phase cells (21). In our study even applying low-dose protocols the differences observed after 1 month of survival between areas located close to or far from the chains do suggest that a certain rate of cell delivery could occur. In conclusion, the striking structural plasticity observed in rabbit, compared with the closely related rodents, supports the hypothesis that the genesis and migration of new cells from periventricular germinative layers could be greater in more complex mammals, as proposed (9, 10).

We thank G. Rougon for anti-PSA-NCAM antibody, G. Zanutto for expertise in graphics, and A. Mannelli for advise in statistics. This study was supported by Fondo per gli Investimenti della Ricerca di Base and Compagnia S. Paolo.

1. Gould, E., Tanapat, P., Hastings, N. B. & Shors, T. J. (1999) Trends Cognit. Sci. 3, 186–192.
2. Lois, C. & Alvarez-Buylla, A. (1994) Science 264, 1145–1148.
3. Bonfanti, L. & Theodosis, D. T. (1994) Neuroscience 62, 291–305.
4. Rousselot, P., Lois, C.&Alvarez-Buylla, A. (1995) J. Comp. Neurol. 351, 51–61.
5. Lois, C., Garcia-Verdugo, J. & Alvarez-Buylla, A. (1996) Science 271, 978–981.
6. Peretto, P., Merighi, A., Fasolo, A. & Bonfanti, L. (1997) Brain Res. Bull. 42, 9–21.
7. Kornack, D. R. & Rakic, P. (2001) Proc. Natl. Acad. Sci. USA 98, 4752–4757.
8. Pencea, V., Bingaman, K. D., Freedman, L. J. & Luskin, M. B. (2001) Exp. Neurol. 172, 1–16.
9. Gould, E., Reeves, A. I., Graziano, M. S. A. & Gross, C. G. (1999) Science 286, 548–552.
10. Gould, E., Vail, N., Wagers, M. & Gross, C. G. (2001) Proc. Natl. Acad. Sci. USA 98, 10910–10917.
11. Bernier, P. J., Be´dard, A., Vinet, J., Le´vesque, M. & Parent, A. (2002) Proc. Natl. Acad. Sci. USA 99, 11464–11469.
12. McFarland, W. L., Morgane, P. J. & Jacobs, M. S. (1969) J. Comp. Neurol. 135, 275–368.
13. Kornack, D. R. (2000) Brain Behav. Evol. 55, 336–344.
14. Leonhardt, H. (1972) Z. Zellforsch. Mikrosk. Anat. 127, 392–406.
15. Peretto, P., Merighi, A., Fasolo, A. & Bonfanti, L. (1999) Brain Res. Bull. 49, 221–243.
16. Garcia-Verdugo, J. M., Doetsch, F., Wichterle, H., Lim, D. A. & Alvarez-Buylla, A. (1998) J. Neurobiol. 36, 234–248.
17. Menezes, J. R. L. & Luskin, M. B. (1994) J. Neurosci. 14, 5399–5416.
18. Doetsch, F., Garcia-Verdugo, J. M. & Alvarez-Buylla, A. (1997) J. Neurosci. 17, 5046–5061.
19. Goldman, S. A. (1997) in Isolation, Characterization and Utilization of CNS Stem Cells, eds. Gage, F. H. & Christen, Y. (Springer, Berlin), pp. 43–65.
20. Wichterle, H., Garcia-Verdugo, J. M. & Alvarez-Buylla A., (1997) Neuron 18, 779–791.
21. Cameron, H. A. & McKay, R. D. (2001) J. Comp. Neurol. 435, 406–417.